A rhodopsin is the functional photoreceptor for phototaxis in the unicellular eukaryote *Chlamydomonas*

Kenneth W. Foster*‡§, Jureepan Saranak*‡, Nayana Patel*, Gerald Zarilli†, Masami Okabe†, Toni Kline* & Koji Nakanishi†§

* Department of Pharmacology, Mt Sinai School of Medicine, City University of New York, New York, New York 10029, USA
† Department of Chemistry, Columbia University, New York, New York 10027, USA

Rhodopsin is a visual pigment ubiquitous in multicellular animals. If visual pigments have a common ancient origin, as is believed, then some unicellular organisms might also use a rhodopsin photoreceptor[1,2]. We show here that the unicellular alga *Chlamydomonas* does indeed use a rhodopsin photoreceptor. We incorporated analogues of its retinal chromophore into a blind mutant; normal photobehaviour was restored and the colour of maximum sensitivity was shifted in a manner consistent with the nature of the retinal analogue added. The data suggest that 11-*cis*-retinal is the natural chromophore and that the protein environment of this retinal is similar to that found in bovine rhodopsin, suggesting homology with the rhodopsins of higher organisms. This is the first demonstration of a rhodopsin photoreceptor in an alga or eukaryotic protist and also the first report of behavioural spectral shifts caused by exogenous synthetic retinals in a eukaryote. A survey of the morphology and action spectra of other protists suggests that rhodopsins may be common photoreceptors of chlorophycean, prasinophycean and dinophycean algae. Thus, *Chlamydomonas* represents a useful new model for studying photoreceptor cells.

Chlamydomonas is an aquatic organism of 10 μm diameter with a single eye and two flagella[3] which together guide the swimming cell in its light environment. A coloured quarter-wave-layered eyespot focuses incoming light onto an overlying patch of plasma membrane containing $\sim 10^5$ receptor pigment molecules and also prevents light from passing through the cell to the receptor pigment[2]. As the cell rotates while swimming, its eye conically scans a pattern of light which modulates conductance changes that control the steering of its flagella, thus forming a simple, but nevertheless complete visual system. All the essential elements of the photoreceptor cells of a multicellular animal are present[2].

Although there are many light-sensitive pigments, particularly in protists[4], the receptor pigments in the eyes of all multicellular animals studied so far contain 11-*cis*-retinal as the chromophore; in addition, some freshwater fish and amphibians use 11-*cis*-3,4-dehydroretinal as a second chromophore. We used the following rationale to check for the presence of a retinal chromophore in *Chlamydomonas*. If a retinal moiety were the chromophore, replacing it by other retinal analogues would shift the action spectrum (the relative sensitivity of the cells to different wavelengths of light) compared with the natural pigment; such a shift in action spectrum would prove the incorporation and function of retinal. Nonspecific binding of retinals to protein would not produce the anticipated shifts. The behaviour used to test the photoreceptor response was that of phototaxis[2,5]—the swimming of an aquatic cell towards or away from light.

Numerous retinal analogues have been bound to bovine opsin and bacteriorhodopsin *in vitro*[6-9] to give pigments absorbing at different wavelengths of light. At least four analogues have recently been shown to shift the behavioural action spectrum of *Halobacterium*[10,11] and a similar rationale using a riboflavin analogue was applied to determine the nature of the chromophore for phototropism in the fungus *Phycomyces*[12].

As with the *Phycomyces* studies in which a riboflavin auxotroph was used[12], we used a blind mutant incapable of synthesizing retinal in the dark to measure incorporation of analogues. As any mutant blocking carotenoid synthesis would also block retinal synthesis, we surveyed all carotenoid mutants we could obtain; as hypothesized, these are blind compared with wild type. We chose the mutant FN68 (Car-1) because of the comparative slowness of its light induction of carotenoids (K.W.F *et al.*, in preparation) and its 1,000–10,000-fold increased threshold sensitivities relative to wild type (compare Fig. 1*B*, *C* with *D*). The carotenoid biosynthesis of the mutant[13] is blocked in the dark at a step before phytoene. The mutant is negatively phototactic, that is, it normally swims away from light. The wild type (for carotenogenesis) (Car^+ agg^- cell, designated FN13) was a negatively phototactic strain (derived from culture 806 of *Chlamydomonas reinhardtii* 137c(−); given by Robert Smyth).

We used threshold measurements of phototaxis (Fig. 1) to determine the sensitivity of the cells to a particular colour of light. The sensitivity or reciprocal of the threshold was plotted as a function of wavenumber (wavelength^{-1}) to give a phototaxis action spectrum for each analogue tested (Fig. 2*A*, *a*–*g*). Peaks were determined by fitting the data to a standard curve[14]. As in other animals, *trans*-retinol (vitamin A) and β-carotene function as well as retinal, while retinoic acid has no effect.

To provide a standard to determine the effect of the protein environment on a retinal analogue, a simple reference environment was needed. As it is known that the retinal in other rhodopsins is attached to the protein as a protonated Schiff base (SBH^+), the absorption of the analogue in that form, attached to a small compound such as *n*-butylamine in the solvent methanol, provides a useful reference. The difference (in wavenumber) between the absorption maximum of SBH^+ in methanol and those of the pigments has been defined as the opsin shift[15]. The action spectra maxima for *Chlamydomonas* are not only shifted towards the red away from the reference maxima provided by the protonated Schiff bases (SBH^+), but the trends of these opsin shifts (Fig. 3) are very similar to those encountered for bovine rhodopsins. The opsin shifts from the SBH^+ model vary over a narrow range, with the 9-*cis* analogues having a smaller opsin shift than the 11-*cis* analogues. In contrast, the shifts observed here are markedly different from those encountered with bacteriorhodopsin, which, unlike visual pigments, absorb at 570 nm and only accept *trans*- and 13-*cis*-retinals[16]. The natural or light-induced action spectra maximum for *Chlamydomonas* is at 503 nm, whereas the maxima resulting from *trans*- and 11-*cis*-retinal incorporation are at 505 and 501 nm, respectively (Fig. 2). As these values are within experimental error, it is likely that the retinals are isomerized in the dark (to 11-*cis* by an isomerase?). However, the maximum at 488 nm caused by incorporation of 9-*cis* is outside the range of error and parallels the 485 nm maximum of bovine 9-*cis* rhodopsin. These findings suggest that *Chlamydomonas*, a chlorophycean, has a pigment homologous to bovine rhodopsin. We suspect the existence of rhodopsins in other algae also (Fig. 4). These pigments show a variation in their maximum absorption wavelength, from 457 to 493 nm, which implies a similar variety of chromophore environments to those in multicellular animals. Although they are probably all rhodopsin-like pigments, the nature of the chromophores in the Prasinophyceae and Dinophyceae remains to be proven.

Our results involving incorporation of retinal analogues have established *Chlamydomonas* as a viable model for studies of rhodopsin photoreceptors. A major advantage of this system is that it is already widely used for the study of basal bodies[17], circadian rhythms[18,19] and flagellar architecture and function[20,21,38], among others. Furthermore, the visual pigment and ionic processing elements are readily accessible as they lie in the plasma membrane at the surface of the cell. The versatility of this genetically well-studied microorganism for the study of photoreception, together with the apparent close homology of its photoreceptor cells to those of multicellular organisms, make it an excellent model. Use of this simple unicellular system

‡ Present address: Physics Department, 201 Physics Building, Syracuse University, Syracuse, New York 13210, USA.
§ To whom reprint requests should be addressed.

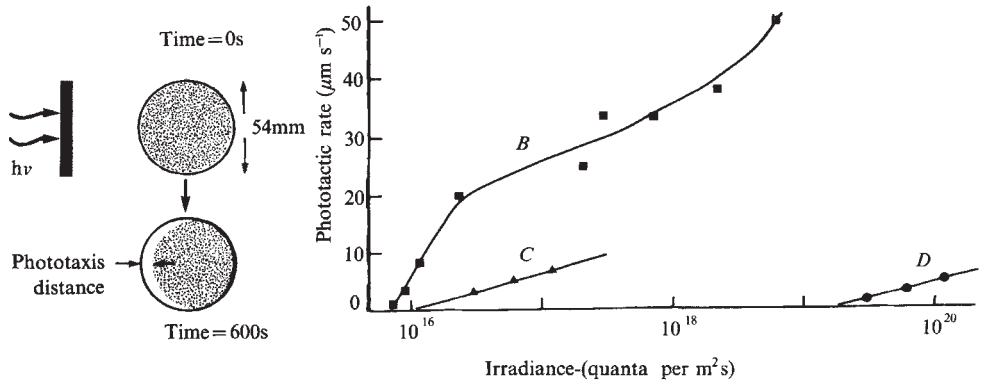

Fig. 1 *A*, The experimental set-up at time 0 and at 600 s. *B–D*, Dose–response curves, using 540 nm light with: *B*, FN13 cells (normal for carotenoids); *C*, FN68 cells and added 11-*cis*-retinal (25 μM); and *D*, FN68 cells without any added retinal. **Methods:** FN68 cells were taken from slant cultures and grown on plates (salt, acetate Bacto-tryptone media with no yeast)[23]. These cells were transferred to HSM liquid (9.3 mM NH_4Cl, 81 μM $MgSO_4$, 0.1 mM $CaCl_2$, 8.27 mM K_2HPO_4, 5.3 mM KH_2PO_4, 15 mM Na acetate, plus trace elements[24]) and grown for 5–7 days in the dark at 18 °C. These vegetative cells were converted to gametes by nitrogen starvation in NMM (81 μM $MgSO_4$, 0.1 mM $CaCl_2$, 4.13 mM K_2HPO_4, 2.65 mM KH_2PO_4, plus trace elements[24]). On the day before the experiment, vegetative cells were centrifuged out at 1,500 r.p.m. for 3 min. The pellets were washed two or three times with NMM and resuspended in NMM to a concentration of $5–7 \times 10^6$ cells ml^{-1}. To the final NMM and cell suspension 25 μM of each retinal analogue and 0.025% α-tocopherol (as an antioxidant) were added. There was a dose-related effect of the analogues, and 25 μM was the lowest concentration that resulted in nearly full recovery with the most effective analogues. All analogues were transferred to methanol solvent immediately before addition to the cells. α-Tocopherol was also dissolved in methanol. The final concentration of methanol in the cell suspension was always <0.5%. Cells were left overnight for gametes to develop and incorporate the analogues. All cells were checked for motility and bacterial contamination. 4–5 ml of the cell suspension were poured into 54 mm diameter polystyrene Petri plates and placed at various distances from a stabilized quartz-iodide light source, the colour of which was selected with a series of interference filters. As the same set of filters was used for each analogue, the error in the comparative data is very small. To ensure a high degree of accuracy, two interference filters in series were used on the rapid fall-off in response to the red. Each light condition was measured with a 400 series Photodyne radiometer calibrated to ±5% for each wavelength. The energies were converted to absolute irradiances and corrected for the small amount of plate absorption. To measure action spectra, dose–response curves of phototactic rate versus light intensity were obtained. The distance travelled by the trailing edge of phototactic cells was measured for a 600-s period. Any effects of light scattering were minimized as light passed through the clear region created by cells swimming away from the light. The amount of opsin available may differ from day to day and the absolute sensitivity at all wavelengths may be changed; therefore, a complete action spectrum for one analogue was determined for one set of cells in one day. A control (undoped cells) was always included and measured for phototactic threshold. The procedure was repeated on a second or third day, if necessary, and all data points plotted with a common symbol for each day's set of data, as shown in Fig. 2. Unfortunately, in our mutant some induction of carotenoid and retinal synthesis (K.W.F. *et al.*, in preparation) occurs in the dark in the presence of retinals and retinal oxidation products (as also found in *Phycomyces*)[25]. However, we minimized oxidation by limiting exposure to light and oxygen and we added the analogues in optimum amounts; thus chemical induction did not interfere with out experiments. The slopes of the dose–response curves vary with wavelength as the conical scanning mechanism (see ref. 2 for details) results in a signal proportional to the magnitude of contrast modulation, which varies with wavelength. Therefore, we used the threshold for phototaxis rather than the intensity to give a standard response. Using this method, the presence of low concentrations of analogues, which contribute <0.001 absorbance units to the contrast modulation, has no effect on the action spectra. For threshold, we used the linear extrapolation to zero response, on a linear plot of phototactic rate as a function of the log of light intensity.

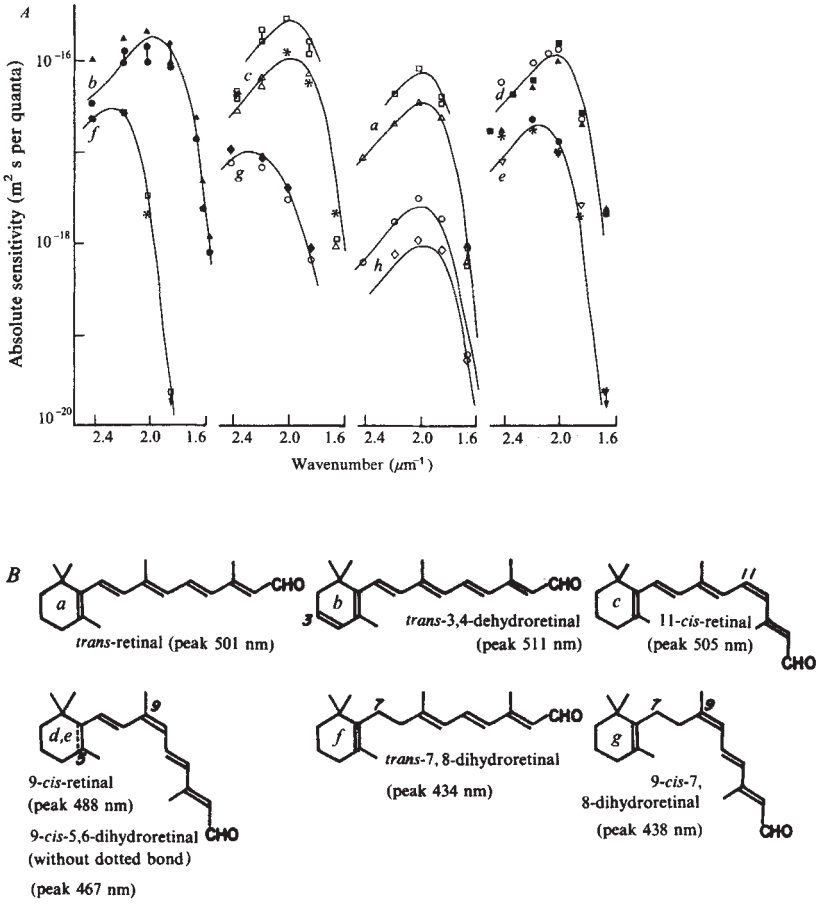

Fig. 2 *A*, The action spectra for different incorporated analogues. *B*, The structure and excitation maxima of the analogues: *a*, *trans*-retinal (peak 501 ± 5 nm); *b*, *trans*-3,4-dehydroretinal[26] (peak 511 ± 2 nm); *c*, 11-*cis*-retinal (peak 505 ± 6 nm); *d*, 9-*cis*-retinal (with dotted bond) (peak 488 ± 5 nm); *e*, 9-*cis*-5,6-dihydroretinal[27] (without dotted bond) (peak 467 ± 5 nm); *f*, *trans*-7,8-dihydroretinal[27] (peak 434 ± 3 nm); *g*, 9-*cis*-7,8-dihydroretinal[27] (peak 438 ± 5 nm); and *h*, light induced at 540 nm for 1.8×10^3 s at an irradiance of 4.2×10^{19} quanta per m^2 per s (upper curve) and 2.5×10^{19} quanta per m^2 per s (lower curve) (peak 503 ± 2 nm). **Methods:** The action spectra were determined by the method described in Fig. 1 legend. log of sensitivity (reciprocal of threshold) on an absolute scale is plotted on the ordinate as a function of the wavenumber (wavelength^{-1}) (μm^{-1}, 10,000 cm^{-1}); when plotted in this way, the shape of the curve of rhodopsin excitation does not change despite shifts of maxima. The ordinate is given an absolute scale to compare the sensitivities of each analogue added at the same concentration. The absolute sensitivity of an analogue is a function of its affinity and quantum efficiency; we did not distinguish between these two parameters in this study. In some cases a second partial curve is drawn through a particular day's data because on that day the analogue's own absolute sensitivity was different. The data were fitted to a standard rhodopsin curve[14] (solid lines) and from this fit the peak wavelengths were obtained. The one exception is 9-*cis*-7,8-dihydroretinal (*g*) for which the curve is distorted by competition with the induced native chromophore (K.W.F. *et al.*, in preparation). To obtain the best estimate of the maxima of the data curve, however, a 1/6 component of natural chromophore was subtracted and the standard curve fitted to the result. In all other cases we are confident of complete dominance of the substitution.

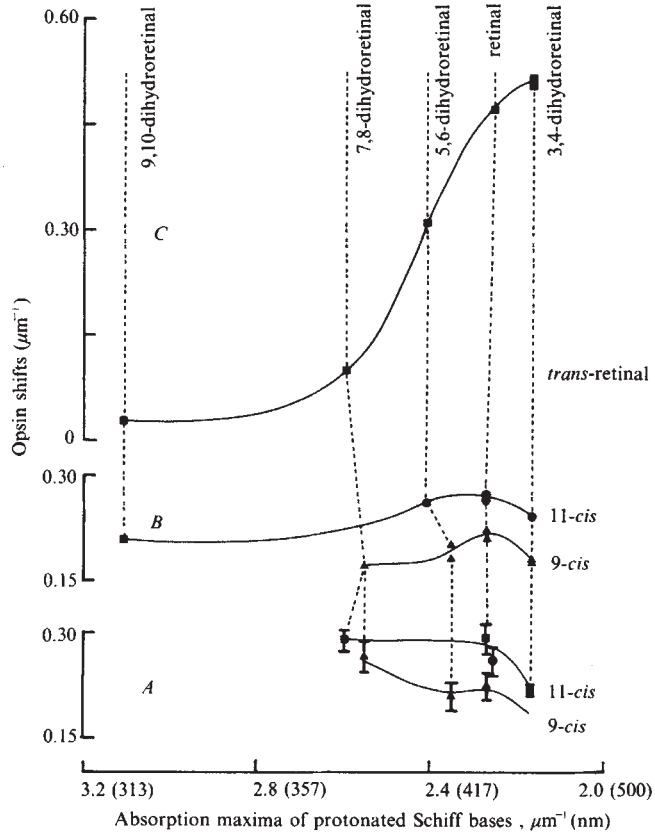

Fig. 3 Chromophore environments of *Chlamydomonas* rhodopsin (*A*), bovine rhodopsin (*B*) and bacteriorhodopsin (*C*). Retinal chromophores in rhodopsins are bound to opsin via a protonated Schiff base linkage, absorption maxima being considerably redshifted from those (in methanol) of protonated Schiff bases formed with *n*-butylamine (SBH^+). This redshift, reflecting the unique rhodopsin protein environment of retinal, expressed in wavenumbers (μm^{-1}, 10,000 cm^{-1}), is defined as the opsin shift[15]. Retinals nonspecifically bound to proteins in the SBH^+ form absorb at the SBH^+ wavelength[28], and in free solution in the UV. In *Chlamydomonas* the action spectra are again redshifted from the SBH^+ form and are fitted so well to the standard rhodopsin curve, so nonspecific protein attachment of retinals has no effect on phototaxis. For *Chlamydomonas* rhodopsin we define opsin shift to include the difference between the maxima of SBH^+ and those of its action spectra. An analogue added *trans* will probably be isomerized by the cell to 11-*cis*, but the SBH^+ values are nearly identical. Opsin shifts of the excitation maxima of *Chlamydomonas* phototaxis (*A*) and of absorption maxima of bovine rhodopsins (*B*) and bacteriorhodopsin (*C*) resulting from incorporation of various analogues are plotted against maxima of the corresponding SBH^+, expressed in μm^{-1}. Data points in the 9-*cis* (▲), 11-*cis* (●) and *trans* (■) series are connected laterally for clarity. The vertical dashed lines interconnect the double bond isomers of respective retinals. The values for the excitation maxima of *Chlamydomonas* are listed in Fig. 2 legend. The values for absorption maxima of SBH^+, bovine rhodopsins (RH) and bacteriorhodopsins (BR) are as follows: *trans*-retinal (*a* of Fig. 2*B*), SBH^+ 443 nm (ref. 29), BR 560 nm (ref. 15); *trans*-3,4-dehydroretinal (*b*), SBH^+ 460 nm (ref. 28), BR 603 nm (ref. 30) or 599 nm (ref. 31); 11-*cis*-3,4-dehydroretinal, SBH^+ 460 nm (assumed to be like *trans* as only a few nanometres different)[28], RH 517 nm (ref. 28); 9-*cis*-3,4-dehydroretinal, SBH^+ 460 nm (assumed to be like *trans*), RH 501 nm (ref. 28) or 500 nm (ref. 32); 11-*cis*-retinal (*c*), SBH^+ 440 nm (ref. 15), RH 498 nm (ref. 28) or 500 nm (ref. 15); 9-*cis*-retinal (*d*), SBH^+ 440 nm (ref. 15), RH 485 nm (ref. 15) or 487 nm (ref. 28); *trans*-5,6-dihydroretinal, SBH^+ 415 nm (ref. 28), BR 476 nm (ref. 15); 11-*cis*-5,6-dihydroretinal, SBH^+ 415 nm (assumed to be like *trans*), RH 465 nm (ref. 28); 9-*cis*-5,6-dihydroretinal (*e*), SBH^+ 425 nm (ref. 15), RH 465 nm (ref. 28) or 460 nm (ref. 15); *trans*-7,8-dihydroretinal (*f*), SBH^+ 385 nm (ref. 15), BR 400 nm (ref. 15); 9-*cis*-7,8-dihydroretinal (*g*), SBH^+ 392 nm (ref. 33), RH 420 nm (ref. 15); and *trans*-9,10-dihydroretinal, SBH^+ 322 nm (ref. 15), RH 345 nm (ref. 15), BR 325 nm (ref. 15).

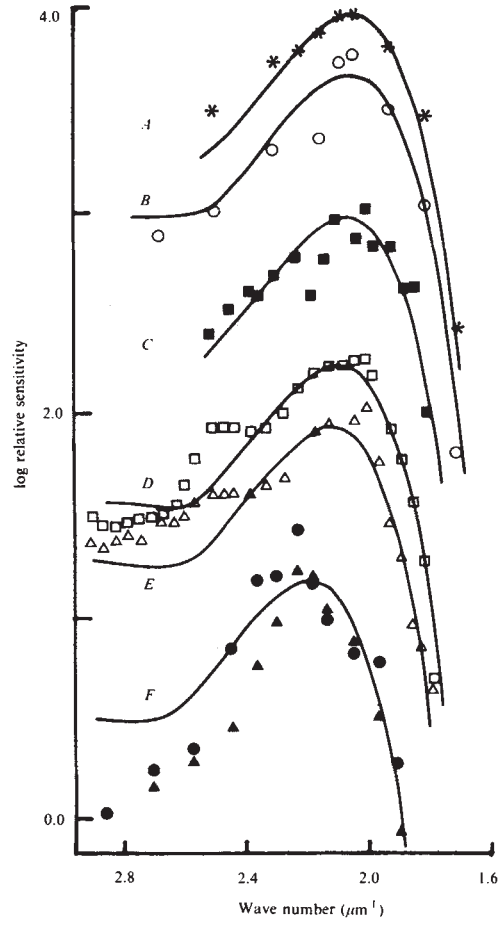

Fig. 4 Action spectra of algae taken from the literature. The most probable homologous characteristic to identify between alga eyes and those of multicellular organisms is an oriented rhodopsin-like protein formed in the plasma membrane regulating ion currents. The use of a photoreceptor at the quarter-wave position overlying a quarter-wave stack antenna in several algal classes (see ref. 2 for details) requires an oriented receptor for optimal functioning. On the grounds of morphology and action spectra, therefore, we have redrawn several action spectra from the literature: log of sensitivity (reciprocal of threshold or quantum efficiency) is plotted as a function of the wavenumber (wavelength^{-1}) (μm^{-1}, 10,000 cm^{-1}) as in Fig. 2*A*. To facilitate comparison, the data have been arbitrarily displaced on the ordinate and the same standard curve[14] has been horizontally shifted to best fit the data from the maximum to the red cut-off of sensitivity. We anticipate significant distortion in the action spectra above 2.3 μm^{-1} (to the violet side of 430 nm) due to activation of photosynthesis. *A*, The 'stop' response (*) of *Volvox aureus* (a chlorophycean) (peak 493 nm)[34]; *B*, the threshold positive phototaxis response (○) of *V. aureus* (peak 490 nm)[34]; *C*, the photoreceptor electrical potential (■) of *Haematococcus pluvialis* (a chlorophycean) (peak 483 nm)[35]; *D*, the threshold negative phototaxis response (□) of *Platymonas subcordiformis* (a prasinophycean) (peak 478 nm)[36]; *E*, the threshold positive phototaxis response (△) of *Pl. subcordiformis* (peak 472 nm)[36]; *F*, the stop response (▲) and positive phototaxis (recalculated) (●) of *Gymnodinium splendens* (a dinophycean) (peak 457 nm)[37].

should allow us to elucidate the active sites of protein interaction; transduction aspects; adaptation; signal processing; membrane, receptor and chromophore biosynthesis and maintenance; nutritional effects on the lipid environment of the receptor; and effects of cell homeostasis.

The use of eukaryotic rhodopsins as visual receptors may indeed be quite ancient and as common in several classes of algae as in higher animals. The use of molecular biology[22] to check for homology between the rhodopsins found throughout these algae and higher animals should prove exciting.

We thank Dr Robert D. Smyth for discussions and the impor-

tant suggestion that a rhodopsin might be the photoreceptor in *Chlamydomonas*. We also thank the NIH for support (grant EY 03760 to K.W.F. and N.P. and grant EY 01253 to K.N.) and the many who lent us equipment to make these experiments possible. W.-Y. Wang (University of Iowa) supplied the FN68 mutant.

Received 22 February; accepted 11 July 1984.

1. Foster, K. W. & Smyth, R. D. *Fedn Proc.* **39**, 2139 (1980).
2. Foster, K. W. & Smyth, R. D. *Microbiol. Rev.* **44**, 572-630 (1980).
3. Ehrenberg, C. G. *Die Infusionthierchen als Vollkommene Organismen*, Leipzig (1838).
4. Song, P.-S. *Photochem. Photobiol. Rev.* **7**, 77-140 (1983).
5. Greuet, C. *Année biol.* **21**, 97-141 (1982).
6. Balogh-Nair, V. & Nakanishi, K. in *New Comprehensive Biochemistry* Vol. 3 (ed. Tamm, Ch.) (Elsevier, Amsterdam, 1982).
7. Balogh-Nair, V. & Nakanishi, K. *Meth. Enzym.* **88**, 496-506 (1982).
8. Kropf, A., Whittenberger, B. P., Goff, S. P. & Waggoner, A. S. *Expl Eye Res.* **17**, 591-606 (1973).
9. Motto, M. G., Sheves, M., Tsujimoto, K., Balogh-Nair, V. & Nakanishi, K. *J. Am. chem. Soc.* **102**, 7947-7949 (1980).
10. Schimz, A., Sperling, W., Ermann, P., Bestmann, H. J. & Hildebrand, E. *Photochem. Photobiol.* **38**, 417-423 (1983).
11. Schimz, A., Sperling, W., Hildebrand, E. & Kohler-Hahn, D. *Photochem. Photobiol.* **36**, 193-196 (1982).
12. Otto, M. K., Jayaram, M., Hamilton, R. M. & Delbruck, M. *Proc. natn. Acad. Sci. U.S.A.* **78**, 266-269 (1981).
13. Wang, W.-Y. *Genetics* **91**, s134 (1979).
14. Knowles, A. & Dartnell, H. J. in *The Eye* Vol. 2B (ed. Davson, H.) 76 (Academic, New York, 1977)
15. Nakanishi, K., Balogh-Nair, V., Arnaboldi, M., Tsujimoto, K. & Honig, B. *J. Am. chem. Soc.* **102**, 7945-7947 (1980).
16. Oesterhelt, D. & Stoekenius, W. *Nature new Biol.* **233**, 149-152 (1971).
17. Huang, B., Ramanis, Z., Dutcher, S. K. & Luck, D. J. C. *Cell* **29**, 745-753 (1982).
18. Straley, S. C. & Bruce, V. G. *Pl. Physiol.* **63**, 1175-1181 (1979).
19. Goodenough, J. E., Bruce, V. G. & Carter, A. *Biol. Bull. mar. biol. Lab., Woods Hole* **161**, 371-381 (1981).
20. Hoops, H. J. & Witman, G. B. *J. Cell Biol.* **97**, 902-908 (1983).
21. Brokaw, C. J. & Luck, D. J. C. *Cell Motility* **4**, 131-150 (1983).
22. Nathans, J. & Hogness, D. S. *Cell* **34**, 807-814 (1983).
23. Nichelson-Guthrie, C. S. & Hudock, G. A. *J. gen. Microbiol.* **129**, 159-165 (1983).
24. Hutner, S. H., Provosoli, L., Schatz, A. & Haskins, C. P. *Proc. Am. phil Soc.* **94**, 152-170 (1950).
25. Eslava, A. P., Alvarez, M. I. & Cerdá-Olmedo, E. *Eur. J. Biochem.* **48**, 617-623 (1974).
26. Hubbard, R., Brown, P. K. & Bownds, D. *Meth. Enzym.* **33C**, 615-653 (1971).
27. Arnaboldi, M., Motto, M. G., Tsujimoto, K., Balogh-Nair, V. & Nakanishi, K. *J. Am. chem. Soc.* **101**, 7082-7086 (1979).
28. Blatz, P. E., Dewhurst, P. B., Balasubramaniyan, V., Balasubramaniyan, P. & Lin, M. *Photochem. Photobiol.* **11**, 1-15 (1970).
29. Erickson, J. O. & Blatz, P. E. *Vision Res.* **8**, 1367-1375 (1968).
30. Tokunaga, F. & Ebrey, T. G. *Biochemistry* **17**, 1915-1922 (1978).
31. Sperling, W. & Schimz, A. *Biophys. Struct. Mech.* **6**, 165-169 (1980).
32. Azuma, M., Azuma, K. & Keto, Y. *Biochim. biophys. Acta* **295**, 520-527 (1973).
33. Honig, B. *et al. J. Am. chem. Soc.* **101**, 7084-7086 (1979).
34. Schletz, K. *Z. Pflanzenphysiol.* **77**, 189-211 (1976).
35. Litvin, F. F., Sineshchekov, O. A. & Sineshchekov, V. A. *Nature* **271**, 476-478 (1978).
36. Halldal, P. *Physiologia Pl.* **14**, 133-139 (1961).
37. Forward, R. B. Jr *J. Protozool.* **21**, 312-315 (1974).
38. Lack, D. J. L. *J. Cell Biol.* **98**, 789-794 (1984).

Co-localization of neurotensin-like immunoreactivity and ^{3}H-glycine uptake system in sustained amacrine cells of turtle retina

Reto Weiler* & Alexander K. Ball

Department of Anatomy and Lion's Sight Centre, Faculty of Medicine, The University of Calgary, Calgary, Alberta, Canada T2N 4N1

Amacrine cells are axonless intrinsic neurones of the vertebrate retina which have cell bodies in the proximal inner nuclear layer and processes contributing to the synaptic network of the inner plexiform layer. They receive input from bipolar, interplexiform and other amacrine cells, and synapse onto these and ganglion cells[1,2]. Amino acid and monoamine transmitters are found in most retinal neurones[3], but peptide transmitters are exclusively located in amacrine cells[4]. Only one neuropeptide, amino acid or monoamine transmitter exists in any single amacrine cell population[4,5]. Coexistence of neuropeptides with classical transmitters has been demonstrated histologically in many neurones of the central nervous system[6], but the physiological relevance of these findings is unknown[7]. We report here evidence of such coexistence in retinal amacrine cells of the turtle, *Pseudemys scripta elegans*. Using combined immunocytochemistry and autoradiography, we have localized both neurotensin-like immunoreactivity and a high affinity uptake system for ^{3}H-glycine to the same amacrine cell, implying that this cell type may use both substances as neurotransmitters. We also present electrophysiological evidence that this type of amacrine cell responds to photic stimulation with a sustained and graded membrane depolarization.

We examined formalin-fixed frozen sections of turtle retina by the peroxidase-antiperoxidase method[8] and found neurotensin-like immunoreactivity in four different amacrine cell types (Fig. 1*a*-*d*)[9,10]. Two of these types occurred more frequently (Fig. 1*a*, *b*) than the other two (Fig. 1*c*, *d*). Type A cells (Fig. 1*a*) are large, with the soma located in the first row of amacrines. They sent a single primary process to the middle of the inner plexiform layer before branching in the proximal half of this layer. Type B cells (Fig. 1*b*) are smaller, with the soma located in the first or second row of amacrines. They stain much more intensely than type A cells. Beaded processes from type B cells extend along the inner nuclear-plexiform layer border for a short distance before dropping to the proximal half of the inner plexiform layer. Both cell types are identical to other neurotensin-like immunoreactive cells described recently[11]. Less frequent neurotensin-like immunoreactive cell types were found in the distal half of the inner plexiform layer (large pyramidal soma, Fig. 1*c*) and the ganglion cell layer, where a thick primary process extended into the middle of the inner plexiform layer before branching (Fig. 1*d*).

Somas of varying sizes in different rows of the inner nuclear layer accumulated ^{3}H-glycine (Fig. 1*e*). Labelling of the inner plexiform layer was diffuse, with no evident banding pattern. Some of the somas which accumulated ^{3}H-glycine also showed neurotensin-like immunoreactivity. We identified these somas as type B cells on the basis of their shape, location and the distribution of their processes. (Somas of type A cells are characterized by their single process, which does not branch until it reaches the proximal inner plexiform layer, whereas type B somas are characterized by several processes which branch immediately after leaving the soma; Fig. 1*a*, *b*.) The diffuse labelling pattern of ^{3}H-glycine uptake within the inner plexiform layer corresponds well with the branching pattern of type B cells. In thin sections (0.5 μm), the co-localization of the two markers in a type B soma was readily identifiable (Fig. 1*f*). Such preparations also confirmed that ^{3}H-glycine uptake and neurotensin-like immunoreactivity was co-localized in type B but not in type A cells (Fig. 1*f*). Although type B cells all accumulate ^{3}H-glycine, they make up only 7% of the ^{3}H-glycine-accumulating cells in the turtle retina. The co-localization of these two markers in one cell implies that this neurone uses both an amino acid and a neuropeptide as neurotransmitters. We also investigated the possible co-localization of neurotensin-like immunoreactivity with [^{3}H]-γ-aminobutyric acid and dopamine accumulation, but evidence of such coexistence could not be established.

In parallel experiments we used intracellular recording and staining techniques to examine the function of type B cells. The processes of most injected amacrine cells ($n = 47$) were either mono- or multi-stratified within the inner plexiform layer, covering 10-70% of it in transverse sections. This branching pattern differed in cells of only one group ($n = 6$), which had somas located in the proximal inner nuclear layer. A few processes from cells of this smaller group left the soma close to the inner nuclear-plexiform layer border, descending through the total inner plexiform layer and branching at different levels with an increasing density of fine branches in the proximal half (Fig. 2*a*). The six injected cells of this type were morphologically homogeneous, differing from one another only in the size of their receptive field. The size and location of the soma of these cells, and the diffuse pattern of their process distribution within

* Present address: Zoological Institute, University of Munich, Luisenstrasse 14, 8 Munich 2, FRG.